

Automatic Multilayer Soil Modelling

Ali Bazaei and Jayson Patrick, Electrotechnik Pty Ltd www.elek.com.au

Abstract— We present an algorithm to automatically obtain horizontally stratified soil models from field data collected by Wenner or Schlumberger electrode configurations. An automatic initial soil model is generated followed by a steepest descent (SD) algorithm is used to converge to a local minimum of an apparent resistivity error criterion. The SD algorithm is repeated several times, each time randomly changing the initial soil model around the best previously obtained soil model. This approach enables the program to obtain a final solution close to the global minimum. The program allows users to select the number of layers after determining the maximum number of layers from field data. The user can also modify the initial automatic model based on a visual assessment.

Index Terms: Electrical earthing and grounding, vertical electrical sounding, Wenner and Schlumberger arrays, multilayer soil model, horizontal stratification, automatic initial soil model, steepest descent iteration, random initialization.

I. INTRODUCTION

Modeling of soil electrical resistivity is essential for design of earthing systems in electrical installations. It is commonly used as a precursor for the designs for electrical substations.

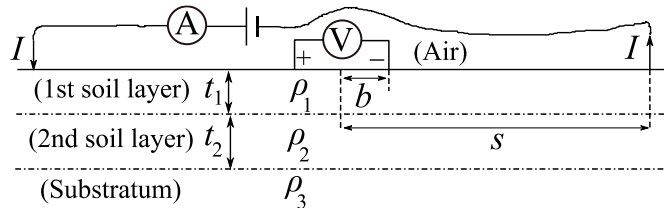


Fig.1. Schematic of linear symmetrical electrode configurations and a 3-layer soil model. Variables t_i and ρ_i refer to thickness and resistivity of i -th soil layer.

II. MULTILAYER SOIL MODEL THEORY

Fig. 1 shows a symmetrical electrode configuration and a horizontally stratified soil model, along with their related parameters. Wenner and Schlumberger electrode configurations are actually special cases of the linear symmetrical case, where electrode spacing values satisfy $s/b = 3$ and $b \ll s$, respectively. This multilayer soil model has an exact integral solution for voltage difference V between potential electrodes due to injected DC current I . The solution assumes that electrode dimensions are small compared to their

spacing values. The integrand is the product of Bessel functions and a resistivity transform function $T(\lambda)$, which is obtained by Pekeris recurrence relations ($\lambda \in [0, \infty)$ is the integral variable in m^{-1}). For a single-layer soil model with constant resistivity ρ , the integral solution reduces to $V = 2\rho Ib / [\pi(s^2 - b^2)]$. This equation is solved for ρ to define apparent resistivity for both field and multilayer soil models.

$$\rho_a = \frac{\pi(s^2 - b^2)V}{2bI} \quad (1)$$

In the Wenner case, $b = a/2$ and $s = 3a/2$, where a denotes electrode spacing and Eq. (1) reduces to $\rho_a = 2\pi aV/I$. In the Schlumberger case, the assumption $b \ll s$ is used to replace ratio of $V/(2b)$ in Eq. (1) by partial derivative of electric potential distribution, during model apparent resistivity calculations. For a multilayer soil model, the integral solution for V can be numerically calculated by linear filtering after transformation of electrode and integral variables into logarithmic scales x and $y = -\ln(\lambda)$, where x is $\ln(a)$ and $\ln(s)$ in Wenner and Schlumberger cases, respectively. The logarithmic transformations convert integral solution of $\rho_a(x)$ into a convolution integral between $T(y)$ (the resistivity transform function in the logarithmic coordinate y) and a function of x independent from soil model parameters, which is considered as an impulse response of a linear filter, called a *resistivity filter*. The resistivity filters for Wenner and Schlumberger electrode configurations have non-causal impulse responses as:

$$h(\eta) = 2e^\eta [J_0(e^\eta) - J_0(2e^\eta)], \quad (\text{Wenner}) \quad (2)$$

$$h(\eta) = e^{2\eta} J_1(e^\eta), \quad (\text{Schlumberger}), \quad (3)$$

where $\eta \in (-\infty, +\infty)$, and $J_0(\cdot)$ and $J_1(\cdot)$ are zero and first order Bessel functions of the first kind, respectively. Figure 2 shows the process of apparent resistivity calculations for a multilayer soil model.



Fig.2. Schematic of numerical calculations for apparent resistivity.

A. Resistivity Filter

The numerical calculation of apparent resistivity is based on a convolution summation between filter coefficients and samples of $T(y)$. The summation is obtained after approximating $T(y)$ by the sum of sinc functions centred at

sampling points and weighted by samples of $T(y)$, based on the Whittaker-Shannon interpolation formula and adopting an identical sampling interval Δy along x and y axes. The filter coefficients are samples of continuous response of resistivity filter to a normalized sinc function of $\text{sinc}(\eta/\Delta y) = [\sin(\pi\eta/\Delta y)]/(\pi\eta/\Delta y)$. Denoting the sinc response function by $S(\eta)$, the filter coefficients are defined as:

$$f_l = S(l\Delta y + x_0 - y_0), \quad l \in \mathbb{Z}, \quad (4)$$

where x_0 and y_0 are the first sampling points on non-negative sides of x and y axes, respectively. The required number of filter coefficients is reduced considerably by considering a shift value between x and y sample points as:

$$x_0 - y_0 = [k - \varphi(f_c)/\pi]\Delta y, \quad k \in \mathbb{Z}, \quad (5)$$

where $\varphi(f_c)$ is the argument of resistivity filter spectrum at cut-off frequency $f_c = 1/(2\Delta y)$ of the sinc function spectrum. This way, filter coefficients are mainly sampled at almost periodic zero crossings of $S(\eta)$ as their abscissae tends to $\pm\infty$. We selected integer k so that the resulting shift is positive and less than Δy . The filter spectrum is a Fourier transformation of the filter impulse response $h(\eta)$. However, numerical calculation of Fourier integral with the expressions mentioned in (2) or (3) in the integrand is very time consuming and may lead to a diverging solution, as shown in Fig. 3 (a). Fortunately, well-behaved smooth functions are available as input-output pairs for Wenner and Schlumberger resistivity filters, such as the following auxiliary functions:

$$T(y) = q\lambda e^{-q\lambda} \Big|_{\lambda=e^{-y}}, \quad (\text{common input function}) \quad (6)$$

$$\rho_a(x) = \left\{ \frac{2a/q}{[1+(a/q)^2]^{1.5}} - \frac{2a/q}{[1+(2a/q)^2]^{1.5}} \right\} \Big|_{a=e^x}, \quad (\text{Wenner}) \quad (7)$$

$$\rho_a(x) = \left\{ \frac{3(s/q)^3}{[1+(s/q)^2]^{2.5}} \right\} \Big|_{s=e^x}, \quad (\text{Schlumberger output}), \quad (8)$$

where arbitrary constant q was assumed to be 1 m. Although the auxiliary input function is not associated with any specific soil model, it generates closed-form expressions at the filter output rather than complicated convolution integrals. An alternative way to find the spectrum of a linear filter is to divide spectrum of filter response by that of the filter input. The task of filter spectrum calculation is now reduced to finding Fourier transforms of auxiliary input-output functions. Integrand of Fourier integrals associated with the auxiliary functions are not only smoother, but also converge rapidly to zero, as shown in Fig. 3(b). Hence, we use these functions to calculate Fourier transforms of the resistivity filters and the required shift between x and y sampling points from Eq. (5).

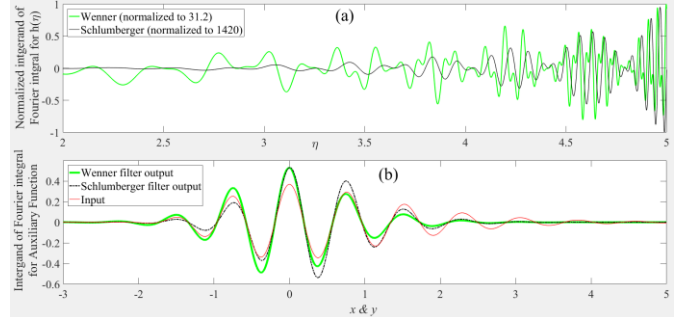


Fig.3. Profiles of integrand functions in cosine terms of Fourier integrals at frequency of 1.3029: (a) for resistivity filters impulse responses, (b) for auxiliary functions. The normalizations in figure (a) refer to division by maximum ordinate magnitude in the indicated range. The selected frequency is cut-off frequency of the sinc function spectrum with $\Delta y = 0.3838$, corresponding to 6 samples per decade along s -axis.

A feasible way to calculate filter coefficients is to use Eq. (4), which involves obtaining $S(\eta)$ from its inverse Fourier transform. Since spectrum of the sinc function is a bandlimited pulse with height Δy and width $|f| \leq f_c$, one needs to calculate filter spectrum only in this interval using those of the auxiliary functions and scale it by Δy before calculating the inverse Fourier integral in the limited frequency range. However, we opted to use an alternative method to obtain filter coefficients, which yields more accurate apparent resistivity values. This method is based on Least Squares, which ends up to a linear system of equations for filter coefficients. Since the coefficient matrix is a symmetric and Toeplitz matrix, we used the recursive algorithm introduced by Levinson in to solve for the filter coefficients. This method does not need any inverse matrix calculations and obtains the solution faster than the Fourier transformation approach. Having found the filter coefficients, samples of apparent resistivity are obtained from resistivity transform samples using a convolution sum as:

$$\rho_{a_k} = \sum_{l_{\min}}^{l_{\max}} f_l T_{k-l} \quad (9)$$

III. INITIAL SOIL MODEL

Like every recursive algorithm, the SD algorithm requires initial values for soil model parameters to start adaptation of the parameters. The approach we take to obtain an initial soil model is based on the observation that apparent resistivity follows soil resistivity with a distance lag, when they share same abscissa for electrode spacing and depth values, as shown by the example in Fig. 4. Note that a step change in soil model resistivity affects apparent resistivity values at both sides of the step abscissa. As in the SD algorithm, the objective in initial

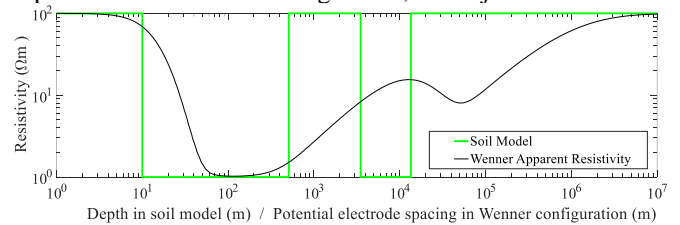


Fig.4. An illustrative example of soil model resistivity versus depth along with the calculated Wenner apparent resistivity versus electrode spacing a .

modelling is to adjust soil layer parameters so that the resulting profile of apparent resistivity is as close as possible to that of field data. Since field data normally consists of a limited number of data points, we use cubic spline data interpolation to obtain missing values of raw data between each pair of adjacent data points. To obtain a smoother profile for the field data, we also enforce endpoint slopes calculated by fitting parabolas to the first and the last triples of raw data points. Having obtained a smooth field data profile, we can numerically identify turning points associated with the field data. Ordinate of the first endpoint is used to assign resistivity of the first soil layer (ρ_1). Minimum value of electrode spacing (a_1) and abscissa of the first turning point (a_1^{TP}) are used to calculate thickness of the first soil layer, using the following empirical formula.

$$t_1 = \begin{cases} \frac{1+a_1}{2}, & \text{if: } a_1^{TP} \geq 1\text{m} \\ a_1, & \text{if: } a_1^{TP} < 1\text{m or no turning point} \end{cases} \quad (10)$$

Coordinates of the first decision point is determined as (t_1, ρ_1) . Resistivity of substratum is determined by the last endpoint resistivity, associated with the largest field electrode spacing. Hence, the last endpoint is the last decision point. The turning points constitute a set of additional decision point candidates to determine intermediate soil layer parameters. The values of thickness and resistivity for intermediate soil layers can be determined from abscissae and ordinates of the turning points. This way, a maximum number N_{\max} is determined for soil layers, which is equal to number of turning points plus 2.

We require the user to select a desired number N of layers not more than N_{\max} , based on an observation of field apparent resistivity profile. In practice, there might be many turning points in the spline due to small fluctuations in measurements or underground imperfections. Hence, we prioritize the turning points and select only the most important $N - 2$ turning points as decision points to be used for specifying initial soil parameters. Turning points with larger distance from average value of field resistivity and smaller distance to average electrode spacing are given more priority.

The foregoing method automatically generates an initial soil model for the user, after selecting number of layers. The user then has the option to modify the initial model an arbitrary number of times by entering arbitrary values for thickness and resistivity of soil layers. This opportunity also enables users to change number of layers, arbitrarily.

IV. AUTOMATIC ITERATIVE INTERPRETATION

After obtaining an initial soil model, we used a combination of steepest descent method and random initializations to reduce the error between field and model apparent resistivity profiles. The SD algorithm iteratively changes to minimize an error criterion defined as average relative error of apparent resistivity. In each iteration, we calculate gradient of the error criterion with respect to soil model parameters and update them in a direction opposite to the gradient vector. Depending on the initial parameter values, the SD method updates soil

model parameters towards a local minimum of the error criterion, which may not be a global minimum.

To increase the chances of convergence to the global minimum, we repeat the SD algorithm for a limited number of times, each time using a new initial soil model. Before each repeat, we record the latest optimum soil model and generate a new initial soil model by assigning random values to soil parameters. The limits of each interval for assigning a random value to each parameter are controlled by the latest available optimal value of the parameter and a constant factor more than 1, denoted *interval factor*. The upper and lower limits of the interval are determined from multiplying and dividing the latest optimal parameter value by the interval factor, respectively. The final solution for the soil model is obtained from the latest recorded optimal solution, when the last repetition of SD algorithm is finalized.

During the optimization, we also prevent unrealistic large or small resistivity values for the first and last soil layers, denoted *endpoint layers*. It is implemented by assigning a constant factor of more than 1 for each endpoint layer, named *resistivity ratio limit*. For each endpoint layer, upper and lower resistivity limits are determined by multiplying and dividing field measured resistivity by the resistivity limit ratio assigned to the endpoint layer. The limits are applied only to resistivity values of the endpoint layers, during each parameter update.

V. ILLUSTRATIVE EXAMPLE

In this section, we present an example to clarify the proposed methods for automatic initial soil modeling and iterative interpretation, mentioned in Sections III and IV, respectively. We adopt the arbitrarily arranged set of field data shown in Fig. 5(a). The resulting spline indicates many turning points ($N_{\max} = 13$), but we assume the desired number of layers is $N = 4$. Hence, two turning points are selected as decision points by the automatic method mentioned in Sec. III. One turning point is selected based on the 4th rank only and the other one based on the final rank. The automatic initial model based on the final ranking is reasonably close to the field data, as shown in Fig. 5(a).

To clarify the importance of the last isolation rank measure in this example, assume all $N - 2 = 2$ decision points are selected only based on the fourth rank. The selected turning points are indicated by the black and red bolded figures in 4th rank column of Table II. In this case, we obtain the automatic initial model shown in Fig. 5(b), which is not close to the field data, adequately. Hence, application of the last isolation rank measure in the final ranking, as proposed in Sec. III, is important for obtaining more adequate initial soil models.

Fig. 5(c) shows results of the proposed automatic iterative interpretation method applied to the automatic initial soil models depicted in Figures 5(a,b). The RMS values of relative error for the final models are 0.1089 and 0.1096 with the 4th and final ranked initial models, respectively, which are close

to each other. The apparent resistivity profiles of the final models are also similar. The final soil model parameters are more notably different, indicating that the resistivity profile has minor sensitivity to some interlayer soil parameters. Considering that the final apparent resistivity profiles almost overlapping, both final solutions should close to actual optimum 4-layer model. In this example, the proposed iterative interpretation method has been successful to converge close to the global minimum even with an inadequate initial model. However, our experience shows that using a more adequate initial soil model increases the change of convergence to a desired model in the iterative interpretation algorithm.

VI.CONCLUSION

A new automatic algorithm for determining an accurate multilayer soil resistivity model from Wenner and Schlumberger field resistivity measurements has been discovered.

The automatic algorithm has been extensively tested and then integrated into SafeGrid™ Earthing Software for accurate modelling of earthing system performance for electrical substations.

REFERENCES

[1]	Nahman, J., and Paunovic, I. (2006). "Resistance to earth of earthing grids buried in multi-layer soil." <i>Electrical Engineering</i> , 88: 281–287
[2]	Saleh, H., and Samsudin, A.R. (2013). "Application of vertical electrical sounding (VES) in subsurface geological investigation for potential aquifer in Lahad Datu, Sabah." <i>AIP Conf. Proc.</i> 1571, 432-437.
[3]	Abdullahi, M.G., Toriman, M.E., and Gasim, M.B. (2015). "The application of vertical electrical sounding (VES) for groundwater exploration in Tudun Wada Kano State, Nigeria." <i>Journal of Geology & Geophysics</i> , 4(1): 1000186
[4]	Emmanuel Hassan (2017). "Groundwater Exploration Using Schlumberger Array Configuration." LAMBERT Academic Publishing.
[5]	Norman Levinson (1946). "The Wiener (Root mean Square) Error Criterion in Filter Design and Prediction", <i>Studies in Applied Mathematics</i> , 25(1-4): 261-278.

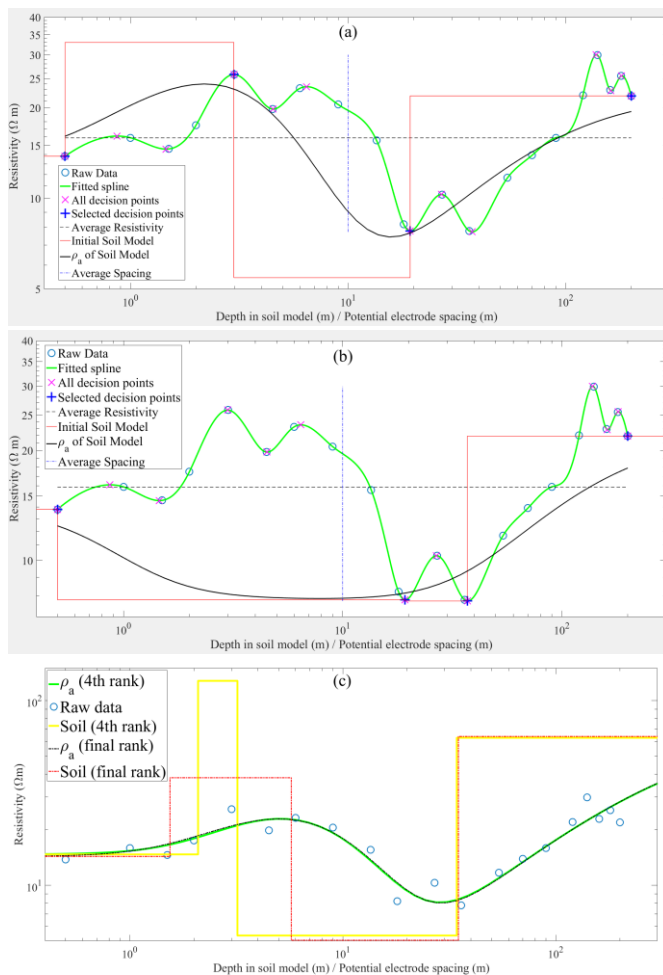


Fig.5. (a) and (b): Automatic initial models obtained for 4-layer soil, based on the final and forth rankings of the turning points, respectively. (c): Final soil models and their apparent resistivity profiles obtained by the proposed iterative interpretation method, using the automatic initial models based on the 4th rank and final rank.